An Agent-Based Model of Heterogeneous Driver Behaviour and Its Impact on Energy Consumption and Costs in Urban Space

Sedar Olmez [1,2,*], Jason Thompson [3], Ellie Marfleet [1], Keiran Suchak [1], Alison Heppenstall [2,4], Ed Manley [1,2], Annabel Whipp [1] and Rajith Vidanaarachchi [3]

1   School of Geography, University of Leeds, Seminary St, Woodhouse, Leeds LS2 9JT, UK; ll16e7m@leeds.ac.uk (E.M.); k.suchak@leeds.ac.uk (K.S.); e.j.manley@leeds.ac.uk (E.M.); gy14aw@leeds.ac.uk (A.W.)
2   The Alan Turing Institute, 2QR, John Dodson House, 96 Euston Rd, London NW1 2DB, UK; alison.heppenstall@glasgow.ac.uk
3   Transport, Health and Urban Design Research Laboratory, The University of Melbourne, Grattan Street, Parkville, VIC 3010, Australia; jason.thompson@unimelb.edu.au (J.T.); rajith.vidanaarachchi@unimelb.edu.au (R.V.)
4   School of Social & Political Sciences, University of Glasgow, Adam Smith Building, Bute Gardens, Glasgow G12 8RT, UK
*   Correspondence: solmez@turing.ac.uk

Abstract: By 2020, over 100 countries had expanded electric and plug-in hybrid electric vehicle (EV/PHEV) technologies, with global sales surpassing 7 million units. Governments are adopting cleaner vehicle technologies due to the proven environmental and health implications of internal combustion engine vehicles (ICEVs), as evidenced by the recent COP26 meeting. This article proposes an agent-based model of vehicle activity as a tool for quantifying energy consumption by simulating a fleet of EV/PHEVs within an urban street network at various spatio-temporal resolutions. Driver behaviour plays a significant role in energy consumption; thus, simulating various levels of individual behaviour and enhancing heterogeneity should provide more accurate results of potential energy demand in cities. The study found that (1) energy consumption is lowest when speed limit adherence increases (low variance in behaviour) and is highest when acceleration/deceleration patterns vary (high variance in behaviour); (2) vehicles that travel for shorter distances while abiding by speed limit rules are more energy efficient compared to those that speed and travel for longer; and (3) on average, for tested vehicles, EV/PHEVs were £233.13 cheaper to run than ICEVs across all experiment conditions. The difference in the average fuel costs (electricity and petrol) shrinks at the vehicle level as driver behaviour is less varied (more homogeneous). This research should allow policymakers to quantify the demand for energy and subsequent fuel costs in cities.

Keywords: agent-based model; electric vehicles; traffic simulation; energy intake; urban environment; fuel costs; public policy

1. Introduction

According to [1], by 2050, 70% of the world's population will live in urban areas, accounting for roughly 6.3 billion people. Battery-powered electric vehicle sales increased from 5.3 million sales in 2019 and are projected to reach over 39.9 million units by 2030 [2]. Given that the majority of people live in urban areas and infrastructure development is targeted at these areas [3], it could be assumed that the majority of electric vehicles (EVs) will be driven in these areas. An environmental benefit that EVs present is the ability to consume energy from renewable energy sources (e.g., wind turbines and solar). Furthermore, the total energy use among EVs is 3.4 times lower than ICEVs that rely on petroleum, diesel or gas, which emit CO_2 that is harmful for the environment. During a well-to-wheel (WTW) analysis of ICEV and EV efficiency, Ref. [4] found that EVs, when

using renewable energy, can reach an efficiency level of 40 to 70% depending on the location and environmental factors. In contrast, gasoline- and diesel-powered ICEVs had an WTW energy efficiency of 11–27% and 25–37%, respectively. Almost all vehicle manufacturing companies have started building and testing EV/PHEVs for the commercial market [5,6]. Governments are facilitating benefits to persuade people to replace ICEVs with EVs through economic incentives or legislation. However, not all countries have renewable technology to power these vehicles; some countries, such as China, still depend on coal to power the majority of their electric grid infrastructure [7,8]. In Australia, only 24% of electricity is generated from renewable sources [9]. In their review of EVs and their impact on the climate, Ref. [10] found that vehicles using electricity from sources with lower global warming potentials (GWP) [11] are better than ICEVs. In contrast, Ref. [12] found it was counterproductive to promote EV uptake in countries where electricity is produced from fossil fuels. The statistics mentioned above reaffirm the need to explore the impact these technologies have on future cities.

This study demonstrates how agent-based modelling (ABM) can be harnessed to quantify energy demand in cities from electric-powered vehicles at various spatio-temporal resolutions. To test the model, two variables are configured across multiple test scenarios to demonstrate the subtle differences in outcomes. These variables are the speeding behaviour (known as adherence to speed limits) and the number of vehicles on the street network (density of vehicles). Through experimentation, we show that individual vehicle behaviours and the number of vehicles on the street network impact the total energy usage (the amount of energy required by the vehicles to complete their drive cycle in kWh). Drive cycle is defined as a series of data points representing the speed of a vehicle versus time.

This article contributes an energy calculation extension (Figure 1) which can be used in conjunction with the agent-based model [13] to quantify EV energy usage. While the focus is centred around electric-powered vehicles, to demonstrate the effectiveness of the model, we illustrate how ICEV vehicles can also be incorporated by converting energy to petrol (L/km), allowing a direct comparison between individual-level behaviours/patterns using two types of vehicles and their relative impact on costs and efficiency. The novelty of this article is three-fold. Firstly, an agent-based method for quantifying energy demand from vehicle behaviour at the individual level is presented. Secondly, heterogeneity among driver behaviour and road characteristics is included, directly impacting the energy required, which is the case in the real world. Finally, the proposed model enables practitioners to quantify the potential energy costs these vehicles incur and compare scenarios such as high traffic to low traffic densities. For clarity, driver behaviour is defined as the interactions of the human driver and the impact those interactions have on the vehicle being driven. This includes, for example, the driver's foot dynamics and its impact on acceleration [14]. This is represented as the speed limit adherence and non-speed limit adherence behaviours, enhancing heterogeneity.
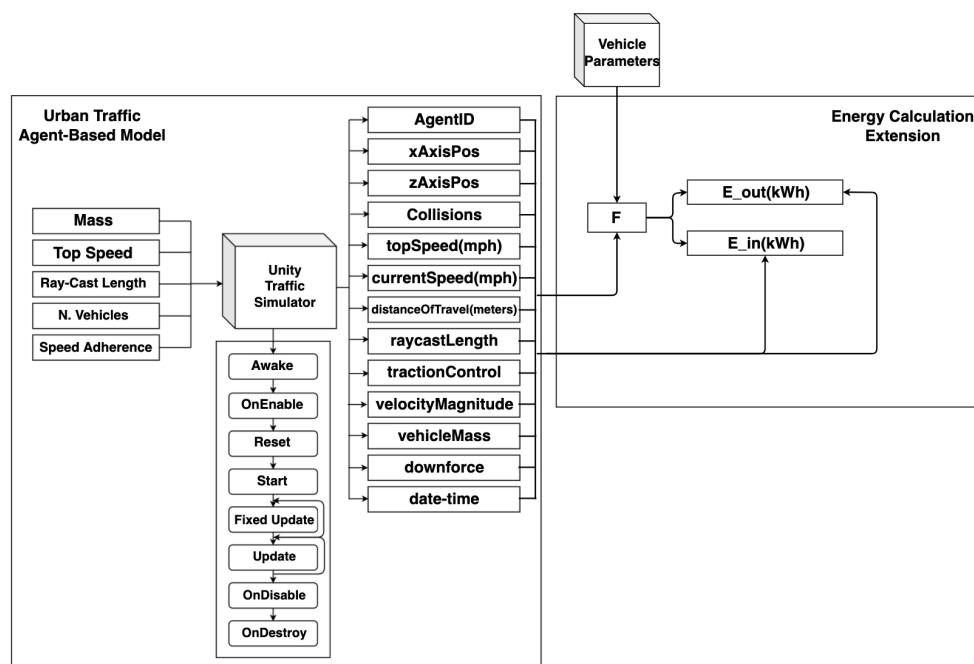
Figure 1. Workflow diagram depicting processes the UTS undergoes during run-time including the Energy Calculation Extension.

2. Background

A traffic system is characterised by multiple individual actors (e.g., drivers) and a street network made up of individual rules characterised by (for example) traffic lights and posted speed limits. Given this system's individual-level components, it is amenable to being studied using individual-based modelling methods. According to [15], individual-based modelling refers to simulation models that treat individual entities as unique and discrete elements with at least one property (e.g., age, height, speed), and these properties change during the life cycle of the entities. Therefore, in this study, vehicles can be thought of as individual heterogeneous entities with their properties and rules, while the urban street network is the environment within which these vehicle entities are observed.

Agent-based modelling (ABM) is an individual-based modelling method. It provides the means to plan, design and experiment with micro-heterogeneous agents in an artificial, computational environment. ABMs have been utilised in various domains to explain complex phenomena such as those that occur in crime [16,17], ecology [18–20], economics [21,22], sociology [23,24], geography [25,26] and transportation [27,28]. One advantage of using ABMs is that they are able to represent a richer and more detailed set of individual actors leading to potential policy alternatives and outcomes compared to the alternative, statistical models [29].

Several agent-based models have focused on electric vehicle research. Ref. [30] developed an agent-based model that measured consumer needs and decision strategies by policymakers to shift from ICEVs to EVs. They found that effective policy requires a long-lasting implementation of a combination of monetary, structural and informational measures. Similarly, Ref. [31] developed a spatially explicit agent-based vehicle consumer choice model to identify the various influences that can affect the uptake of PHEVs. The study found that providing consumers with ready estimates of expected lifetime fuel costs associated with other vehicle types, including the rise of petrol costs, can generate preferences for purchasing EV/PHEVs over ICEVs.

Several studies have also explored the total cost of ownership between EVs and ICEVs from a consumer perspective to quantify the economic differences in ownership between vehicle types. Findings differ geographically due to international differences in the price of petrol, diesel, and electricity. In a study focused on New Zealand, Ref. [32] estimated

that the per-kilometre cost of ownership (PCO) for a used EV was twelve percent lower than that of a used petrol-powered car over twelve years (25.5 NZ cents and 31.5 NZ cents for petrol vehicles). Although this study primarily focused on the differences in fuel costs, others have included additional factors such as insurance, vehicle depreciation and maintenance. Ref. [33] analysed these factors between 1995 and 2015 and found that in the UK, USA and Japan, owners of both mid-size battery EVs (BEVs) and hybrid EVs (HEVs) incurred lower costs than owners of ICEVs during the same period.

Fuel and electricity prices need to be estimated beyond the current year to provide insight into the future costs in ownership between EVs and ICEVs. This is difficult given the inherent fluctuation in oil and electricity markets. However, when investigating the relationship between oil and electricity prices, Ref. [34] found that the Engle–Granger co-integration method identified a short-term relationship between these fuel types. Ref. [32], on the other hand, assumed that changes in fuel prices would follow the past decade trends, which exhibit a 1.4% per year increase for petrol and a 1.1% increase for electricity. Their findings for New Zealand, therefore, cannot be easily transferred to an international context because user-end electricity costs differ drastically between countries, with higher household electricity costs in Germany, Denmark and Italy and lower costs in Mexico, Korea, and Turkey [35]. Such discrepancies in findings are reflected in international studies [36], which found that without subsidies, limited models of BEVs and HEVs incurred lower running costs than ICEVs at the time. Given the complexities mentioned above of integrating fluctuating costs of petrol and electricity into our analyses, we will use the most recent cost of electricity kWh per km and petrol per L/km in the UK.

As the discussion above indicates, EV modelling is a relatively new area of research. Prior studies also focused on a narrow set of issues such as market penetration and charging infrastructure, which may ultimately be driven by price considerations made by individual prospective owners. We, therefore, contend that planning and developing forecasts of electric energy consumption alongside pricing in urban street networks is of critical importance because electricity demand and pricing will influence uptake.

3. Model Description

This section describes the agent-based model adopted for this study. The overview design and details (ODD) protocol will be utilised to explain all aspects of the model [37].

3.1. Purpose

The agent-based model used in this research is the 3D Urban Traffic Simulator (UTS) in Unity [13]. The model was developed to allow researchers to simulate hypothetical vehicle drive cycle scenarios in a 3D urban environment. The model delivers heterogeneous autonomous vehicle agents with granular features such as mass, velocity and traction control. Similarly, the road network is designed around a built-up environment that contains all the characteristics of a dense urban street network with varying speed limits and intersection rules adopted from the UK Speed Limits [38]. Lastly, the model was used by researchers looking at how driver behaviour impacts collision rates [28].

3.2. Variables

The model requires input parameters to run an experiment and produces output results for later analysis. The parameters that can be tuned are listed in Table 1.

The model has two entities: the vehicle agents and the model environment in which these agents are based. The vehicle parameters are:

- The vehicle mass parameter, drawn from a random uniform distribution between 1000 and 3000 kg (inclusive), allows the model to simulate a wider variety of vehicle types, from sedans to SUVs and hatchback. The rationale behind this distribution was to try intersect the EV and ICEV vehicle types, which larger vehicles such as vans or trucks are not part of; the model distributes vehicles arbitrarily across the environment with varying weights (source [39]).

- The top speed measure is between 30 and 45 mph (48, 72 km/h) and is only applied to vehicles that do not adhere to speed limits. This measure is applied only if Speed Adherence is ≥1 (source [40]).
- The gap acceptance parameter can be between 1 to 10 for each vehicle. The variable assigns a distance between two vehicles in meters. This ensures a wider variety of visual impairment is captured as some people with healthier eyes keep a fair distance from vehicles in front usually adhering to the 2-s rule compared to people with worse vision. Furthermore, the distance had to be relative to the average road distance in the model.

The environment-specific parameters are:

- The number of vehicles generated in the model, N. This can be between 1 and 500. However, this can be adjusted depending on the compute power accessible. The hardware accessible at the time of writing this article could only efficiently simulate up to 500 vehicles in 3D space while yielding valid results (refer to the Conclusions section for more on this limitation).
- The speed adherence variable can be between $0 \leq x \leq N$. This quantifies the proportion of vehicles that will not adhere to the speed limits applied to the road they are driving on.
- The urban road network consists of 1295 roads which vehicles drive on and 354 intersections which consist of traffic rules (Algorithm 1, Ref. [28]). The road network has been designed to depict a small urban town.

The parameters above are used to produce output variables that observe various data points at every step of the simulation run, collecting individual-level data from each vehicle. Table 2 describes the output variables that the model produces.

Table 1. Model entities and parameter values (source: [28]).

Entity	Parameter	Values
Vehicle	Mass	[1000, 3000] (kg)
	Top speed	[30, 45] (mph), [48, 72] (km/h)
	Gap acceptance	[1, 10] (m)
Environment	N. of vehicles	[1, 500]
	Speed adherence	[0, N]
	Roads	1295
	Intersections	354

The ABM outputs thirteen variables that can be used for analysis (refer to Table 2). As the agent ID variable is present, a micro-level analysis of the agent behaviours during model execution (e.g., observing individual drive cycles) can be explored. The collisions variable tracks the number of times a vehicle has collided with another. Top speed is the speed limit associated with the road that the vehicle is driving on, which the vehicle tries to match. However, in scenarios where some vehicles do not adhere to speed limits, this would be a value between 30 and 45 mph (48, 72 km/h). The current speed value is the vehicle's speed at the current time step of the model. The distance of travel tracks the vehicle's distance from the starting position on the road network at each time step in metres. The gap acceptance length is the distance the vehicle keeps from vehicles ahead. The velocity magnitude is a scalar value indicating the rate of motion at that specific time step. The vehicle mass variable assigns a weight to the vehicle between 1000 to 3000 in kilograms. The physics engine requires that every object have a mass assigned to it to ensure gravity is applied. The downforce coefficient is set to 0.1; for this research, it is left at 0.1 to have no impact on the vehicles. Lastly, date-time stamps are included in each row of data recorded such that time-series analysis can be applied. These output data are then used as input to the energy calculation extension, which calculates energy intake and outputs energy-specific data, as seen in Table A1.

Table 2. Model output variables.

Variable	Output Type
AgentID	Integer
xAxisPos	Float
zAxisPos	Float
collisions	Integer
topSpeed (mph)	Float
currentSpeed (mph)	Float
distanceOfTravel (meters)	Float
gapAcceptance (raycastLength)	Integer
tractionControl	Bool
velocityMagnitude	Float
vehicleMass	Integer
downforce	Float
date-time	DateTime

3.3. Model Overview

The agent-based model was developed using the Unity development stack. Unity is a 3D game engine consisting of a rendering and physics system and a graphical user interface. The primary programming language is C#. Unity has received widespread adoption in several industries, including gaming, automotive, and film [41].

The following workflow diagram (Figure 1) describes the processes that the model [13] undergoes during run-time. In addition, the energy consumption calculation extension is also depicted.

The UTS [13] workflow (Figure 1) starts by taking input values for the five variables described in Table 1. The software then resets all settings to launch the simulation scene to render the agents and environment. Once the reset process is complete, the model processes all agents, their starting locations and environment parameters. Next, the model can run each frame, and every change that occurs is captured and stored with a time-stamp in a CSV file. Fixed Update is used to compute physics elements such as vehicle wheels, mass, velocity. Update, on the other hand, computes variables for each frame. The model uses Fixed Update due to the sheer number of physics components involved; these variables are tracked multiple times each frame. Once the user stops the model, the sixteen output variables are saved in a directory, and the model is destroyed (stopped). The output dataset is then used as input to an energy calculation notebook (Figure 1), which uses the outputs to calculate *F* from Equation (A3), with vehicle parameters from Tables 3 and 5. The output from this calculation is then used to calculate Equations (A6) and (A7) (Section 4.1).

3.4. Agent

The vehicles in the model are classed as autonomous agents; the vehicle population is heterogeneous, meaning every vehicle will have varying features. These agents inherit similar characteristics as real-world vehicles; they have four wheels, a steering angle, traction, mass and drag. Each agent applies a set of rules outlined in the article [28].

The rules described in [28] allow autonomous vehicle agents to navigate the environment and act as data collectors. Each vehicle follows the same condition-action rules. However, the parameters vary and depend on the input values from Table 1. These vehicle agents are a simplification of real-world vehicles. Therefore, they are not expected to mimic the actions and behaviours of real-world vehicles perfectly, but they do include the essential behaviours that all vehicles demonstrate, such as stop/start and give-way behaviour.

If a vehicle is not adhering to the speed limits, it can increase its speed between 30 and 45 mph (48, 72 km/h). If vehicle A is ahead of B, B should decrease speed to match vehicle A's speed. When a vehicle arrives at an intersection, if it has the right of way (i.e., on a horizontal lane and no vehicles are on the intersection), it drives through the intersection at 10 mph (16 km/h). If the vehicle is at the intersection and does not have the right of way, it should wait until the intersection is cleared. If the vehicle is at an intersection and does not

have the right of way, and there are no other vehicles at the intersection, the vehicle is free to reduce speed to 10 mph (16 km/h) and drive through the intersection. Lastly, all vehicles that adhere to the speed limit increase or decrease speed to match the road's speed limit.

3.5. Environment

The agents described in the last sub-section require an environment to function within. The UTS [13] deploys an urban street network that is described as a T-type network pattern in [42] which contains similar characteristics as downtown Philadelphia, PA [43] and San Francisco [44]. T-network patterns are like grid-shaped networks but include t-junctions. Several added features such as the eight-lane intersections described in [45] also exist. The street network contains 1295 roads and 354 intersections, arbitrarily generated to cover a small town. The individual roads, speed limits and intersection rules are described in the following Figure 2.
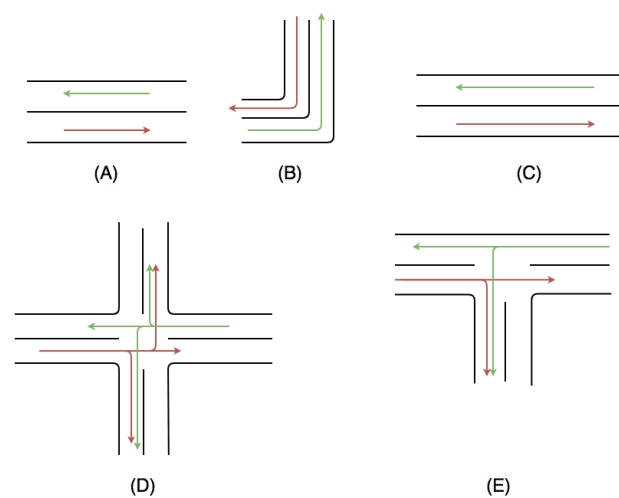

Figure 2. Urban Street Network roads and intersections (source: [28]).

The environment consists of three road types with varying speed limits and intersections with right-of-way rules. The model environment is a simplification of the real world. Therefore, it does not capture all intersection types. However, it does contain the basic characteristics of an urban street network which have also been observed in several cities across the United States [43,44,46]. The vehicles also adhere to stop-go rules (conceptualisation of traffic lights) enforced at junctions. These rules are present in the vehicle's decision-making algorithm [28]. The following list describes each road and intersection in Figure 2:

- (A) A two-way local road with a speed limit of 20 mph (32 km/h);
- (B) A two-way corner road with a speed limit of 10 mph (16 km/h);
- (C) A two-way fixed road with a speed limit of 30 mph (48 km/h);
- (D) An eight-way intersection. Right-of-way is for traffic on horizontal lanes, and the speed limit is 10 mph (16 km/h);
- (E) A two-way t-junction. Right-of-way is for horizontal lanes, and the speed limit is 10 mph (16 km/h).

The speed limits for the three types of roads (Figure 2A–C) were derived from UK government sources such as [40], where urban street networks consist of local 20 mph (32 km/h) and fixed 30 mph (48 km/h) zones; however, corner roads sometimes require lower speeds such as 10 mph (16 km/h) as vehicles require more room to turn. The 'setting local speed limits' report by the UK Government's Department for Transport outlines that most urban streets (roads in built-up areas) have a fixed speed limit of 30 mph (48 km/h). However, for dense areas—usually city centres—this may be designated 20 mph (32 km/h) by local councils to keep pedestrians safe from collisions [28,47].

4. Results

This section will analyse the experiments designed to quantify electric energy consumption across multiple vehicle densities and adherence levels. Once this is achieved, the model will quantify fuel consumption by simulating an ICEV drive cycle as a direct comparator between PHEV/EV and ICEV fuel consumption. The aforementioned comparator experiment will present novel insight by comparing drive cycle, fuel consumption and costs of ICEV and compare these patterns to the alternative PHEV/EV outputs. The output data from the energy calculation extension notebook can be found in Table A1.

Before running the experiments and analysing outputs, the model must be tested against either (1) empirical data, which entails vehicle drive cycle and energy consumption in kWh over km travelled, or (2) model outputs from a different model utilised in research by the research community. Without a baseline comparator, there is no way in knowing if the model utilised in this research, namely [13], outputs energy consumption accurately. Almost all agent-based models are validated using the former or latter processes [17,28,48–52].

The data used to compare model outputs were adopted in the following study [53]. This study utilised German automotive statistics from empirical sources to generate drive cycles of EV journeys using a mathematical model. The variables of interest are kilowatt-hour over distance travelled in kilometres. The specific dataset used contains the drive cycle of 200 vehicles, where input parameters are derived from the statistics mentioned above and the physical properties of vehicles used in Germany [54]. The main drawbacks of this model are:

- That it produces outputs at a time resolution of 15 min; our model, on the other hand, has a time resolution of 1 s. This way, we can capture finer detail such as the impact of traffic lights on acceleration/deceleration and momentary traffic congestion;
- That it only captures trips that are split into commuters and non-commuters. Thus, the modelled scenarios revolve around two profiles of drivers. Our model manipulates the entire system from the street network to traffic rules and vehicles; thus, no single driver profile is modelled, but a heterogeneous set of behaviours are captured.

These factors play an essential role in the electric energy consumption post-simulation run. The main strength of [53] is that variables such as heat transfer, weather, road condition and slope are all introduced as parameters to produce more robust energy consumption results. In our study, we make some basic assumptions, such as: our road surfaces are flat, and no weather parameters are introduced; these variables add complexity to the agent-based model and can hamper computation which, in turn, can affect outputs. We have, however, introduced rolling resistance (Equation (A1)) and braking energy recovery (Figure A1) which both impact electric intake. Adding additional levels of complexity is an area for future development.

4.1. Electric Energy Consumption Calculation

As the vehicle agents are not configured to mimic a specific vehicle, the goal is to adopt parameters from empirical statistics to ensure our findings are consistent with those within the UK given the environmental parameters adopted, such as local and fixed speed limits (Figure 2). Currently, the most popular EV/PHEV in the UK is the Mitsubishi Outlander (source [55]), with over 46,400 units sold as of June 2020. Therefore, this is the chosen vehicle in our analyses. However, the model can be readily adapted to other vehicles and can replicate a heterogeneous fleet.

Equations (A3), (A6) and (A7) were applied to the model outputs to calculate electricity intake:

- For Equation (A3), F is calculated by using the following parameter variables: $\theta = 0$ as the surface area is flat, $C_D = 0.33$, $A = 3.078$ m (where height = 1.71 m, width = 1.80 m), $m = 1925$ kg (Table 3), $a = \frac{\Delta v}{\Delta t}$, where Δv is the velocity change over time period Δt, and lastly, v = velocityMagnitude (Table 2).

- For Equation (A6), E_{out} is calculated by multiplying the output from Equation (A3) with total_distance (d) travelled in meters per second for each agent; see Table 2.
- Lastly, Equation (A7) is calculated by multiplying the output from Equation (A3) (F) with the distance travelled d divided by the engine efficiency $k = 0.65$. E_{in} is then divided by 3.6×10^{-6} to convert from joules to kilowatt-hours (kWh).

Table 3. Vehicle parameters (PHEV).

Parameter	Value
Height (m)	1.71
Width (m)	1.80
k	65% (source [56]) [1]
m (kg)	1925
C_D	0.33

[1] The official engine efficiency statistic is not provided by the vehicle manufacturer; therefore, an average engine efficiency for PHEVs was acquired from the cited academic source.

To compare both emobpy [54] with UTS [13], we ran UTS for one hour, where fifteen vehicles were present. To add complexity, we set five of these vehicles to break speed limits; this allows us to capture the subtle differences between rule followers and rule breakers and their relative energy efficiency and energy consumption over a drive cycle. In comparison, fifteen vehicles were taken from emobpy and plotted against our model outputs.

We aggregated the fifteen vehicles from [13] to five gradient colours to simplify the legend in Figure 3.
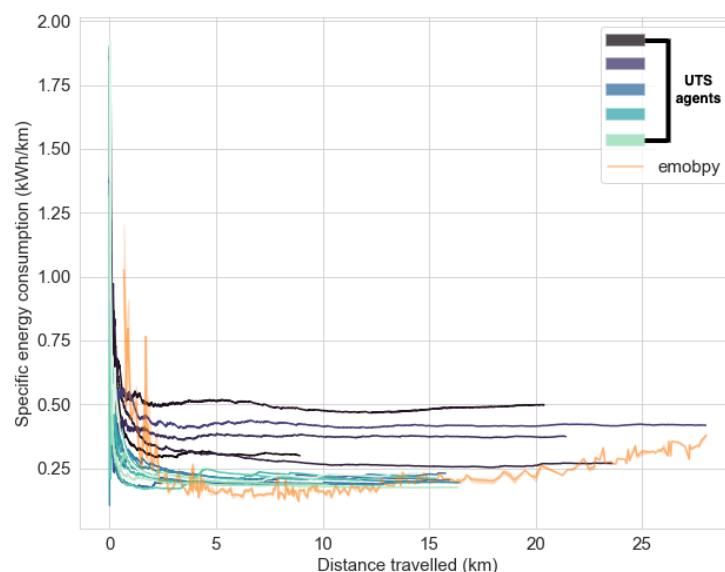

Figure 3. Model output comparison: electric energy consumption (kWh) against distance travelled (km), with 15 vehicles over a 1 h drive cycle (5 vehicles break speed limits).

Figure 3 distinguishes between the rule followers and rule breakers. We can see the clustered lines at the bottom of the graph; these are vehicles that fully adhere to speed limits. On average, these vehicles consumed roughly 0.15–0.25 kWh/km. The five vehicles that broke speed limit rules travelled further as they were speeding and, on average, consumed more energy and were less energy-efficient, as expected. Furthermore, the urban environment has impacted the distances these vehicles could cover (differences in distance travelled). The furthest a vehicle has travelled is 28 km. We also found that the least energy efficient vehicle was consuming roughly 0.50 kWh/km. It is evident that the model outputs from emobpy and UTS are in agreement, where the longer and faster a vehicle drives the

less efficient it becomes. These characteristics of energy efficiency and consumption are evident in empirical literature [57,58].

This small sample shows that the confidence intervals for emobpy are small. This means that vehicles are likely to follow similar drive cycle patterns and configurations, leading to similar energy consumption outputs. However, due to heterogeneity, our model captures a more diverse range of outputs from the same environment, which is a strength of the ABM approach over standard mathematical models.

The energy consumption (kWh/km) patterns are similar for both emobpy and UTS; see Figure 4. These preliminary results are promising as they show that UTS is capable of producing behaviours of realistic drive cycles of electric vehicle energy consumption that have also been observed in a completely different model [53]. Now that we have shown that UTS produces valid estimates of electric energy consumption, we can devise experiments to quantify the effects of speed limit adherence and vehicle density on electric energy (kWh/km) and petrol consumption (L/km).
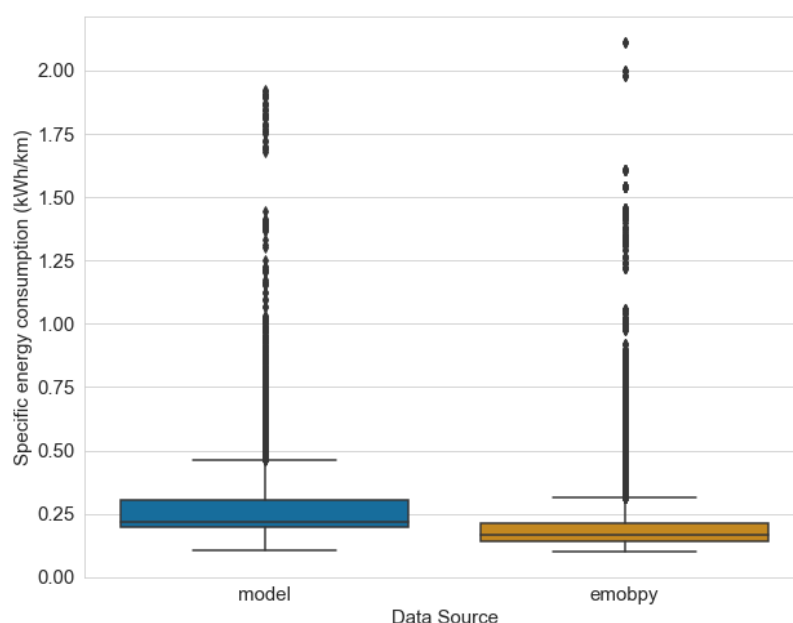

Figure 4. Model Output comparison: electric energy consumption (kWh) for both UTS (model) [13] and emobpy [54].

4.2. Experiments

Due to the computational processes required to render 3D vehicles through space and time [13] and the hardware capacity at hand, nine computationally cheaper experiments were designed. The independent variables were density and adherence to speed limits. These experiments are formally described in Table 4.

Table 4. Experiment conditions.

Variable	Low Adherence	Medium Adherence	High Adherence
Low Density	Condition 1, 10 vehicles, 10 non-adherence	Condition 2, 10 vehicles, 5 non-adherence	Condition 3, 10 vehicles, 0 non-adherence
Mid Density	Condition 4, 50 vehicles, 50 non-adherence	Condition 5, 50 vehicles, 25 non-adherence	Condition 6, 50 vehicles, 0 non-adherence
High Density	Condition 7, 100 vehicles, 100 non-adherence	Condition 8, 100 vehicles, 50 non-adherence	Condition 9, 100 vehicles, 0 non-adherence

These experiments should, in theory, allow us to explore energy consumption in different environmental and behavioural scenarios. The experimental conditions should yield an array of patterns that quantify energy consumption under these conditions. To explore these data, we produce several visualisations and later interpret outcomes.

As more vehicles adhere to speed limits, we see that the cumulative energy consumption is at its lowest 0.1–2 kWh (Figure 5c,f,i). On the contrary, as more vehicles break speed limits, we see cumulative energy consumption at its highest (Figure 5a,d,g). As density increases, the cumulative energy consumed also increases (Figure 5g,h,i) regardless of speed limit adherence.

As adherence to the speed limit increases, it was observed that the overall distance travelled by vehicles was smaller; thus, energy consumption decreased Figure 6.

According to official Mitsubishi statistics [59], the range of the Outlander (kWh/km) is 0.169. To compare, the outputs in Figure 6 show that as adherence increases (Experiment Conditions 3, 6, 9), the cumulative energy consumed is closer to the manufacturer's statistics. The similarity in high adherence cases and energy consumption compared to official statistics can be explained because these statistics were based on fixed/local speed limits in urban environments and do not account for speeding behaviour or consumption levels resulting from motorway speeds. Furthermore, energy efficiency increases as driver behaviour becomes more homogeneous (high adherence), which is what we would expect to see. These data show that the Energy Calculation Extension notebook seen in Figure 1 enables the UTS [13] to quantify the electric energy consumption, so long as the parameters outlined in Table 3 are provided.
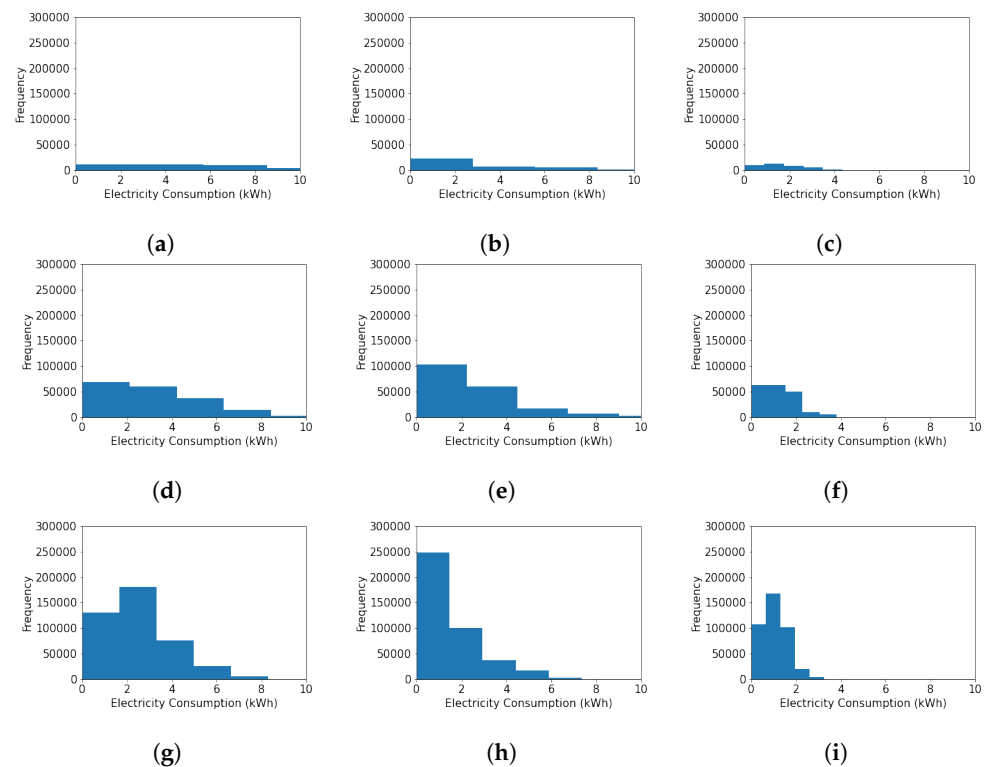

Figure 5. Distribution of the cumulative energy consumption (kWh) for each experiment condition: (**a**) 10 vehicles, 10 non-adherence; (**b**) 10 vehicles, 5 non-adherence; (**c**) 10 vehicles, 0 non-adherence; (**d**) 50 vehicles, 50 non-adherence; (**e**) 50 vehicles, 25 non-adherence; (**f**) 50 vehicles, 0 non-adherence; (**g**) 100 vehicles, 100 non-adherence; (**h**) 100 vehicles, 50 non-adherence; (**i**) 100 vehicles, 0 non-adherence.

To recap, the previous Section 4.1 developed experiments comparing outputs from the UTS [13] to a mathematical model of energy fuel intake, emobpy [53], for validation.

We found the UTS and Energy Calculation Extension notebook Figure 1 produced results consistent with the mathematical model of driver behaviour [53]; see Figures 3 and 4. The subsequent section, across nine experimental conditions, compared the effect that adherence to speed limits and vehicle density had on electric energy consumption by modelling a specific vehicle type (Table 3) and subsequent results (Figures 5 and 6).
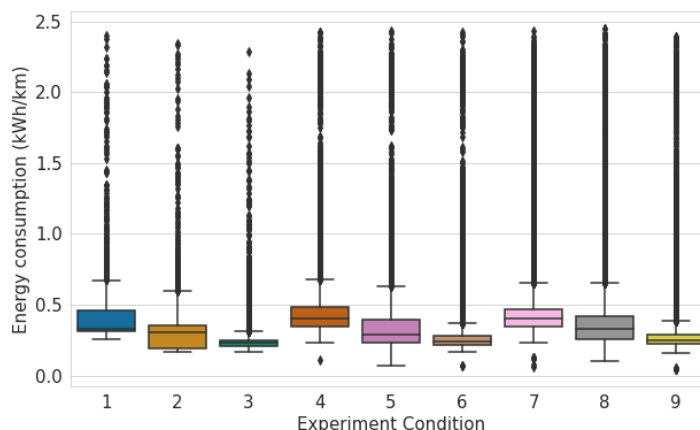

Figure 6. Box plots of energy consumption per kilometer (kWh/km) across all experiment conditions.

4.2.1. Fuel Consumption of Internal Combustion Engine Vehicle Fleet

Following the aims set out in Section 1, to produce estimates of petrol consumption (L/km), an ICEV must be modelled. This process is straightforward, as the UTS is not vehicle-specific; other fuel types such as petrol and diesel can be modelled using the formulae from Appendix A.1.

As previously discussed in Section 4.1, a specific type of vehicle must be identified to model energy consumption. From January 2020 to December 2020, the Ford Fiesta ST was purchased (registered) 49,174 times in the UK, making it the most-purchased ICEV according to [60]; therefore, it was the chosen ICEV. The vehicle parameters can be observed in Table 5.

Table 5. Vehicle parameters (source [61]) (ICEV).

Parameter	Value
Height (m)	1.469
Width (m)	1.941
k	0.33% ([62]) [1]
m (kg)	1635
C_D	0.341

[1] The official engine efficiency statistic is not provided by the vehicle manufacturer; therefore, an average engine efficiency for ICEVs was acquired from the cited source.

Equations (A3), (A6) and (A7) were applied to the model outputs to calculate petrol intake:

- For Equation (A3), F is calculated by using the following parameter variables: $\theta = 0$ as the surface area is flat, $C_D = 0.341$, $A = 2.851$ m (where height = 1.469 m, width = 1.941 m), $m = 1635$ kg (Table 5), $a = \frac{\Delta v}{\Delta t}$ where Δv is the velocity change over time period Δt, and lastly, v = velocityMagnitude (Table 2).
- For Equation (A6), E_{out} is calculated by multiplying the output from Equation (A3) with total_distance (d) travelled in meters per second for each agent; see Table 2.
- Lastly, Equation (A7) is calculated by multiplying the output from Equation (A3) (F) with the distance travelled d divided by the engine efficiency $k = 0.47$. E_{in} is then multiplied by 2.923 to convert joule to gasoline/petrol (L).

To ensure comparability, the experiment conditions in Table 4 will be re-run using the vehicle-specific parameters from Table 5.

As engine efficiency for ICEVs is relatively low compared to EV/PHEVs, the amount of petrol converted to power that moves the vehicle is also low. Roughly 70% of energy is lost during this process [62]. Given the aforementioned, it is likely that the fuel consumption outputs seen in Figure 7 deviate from the true value by some margin.

As expected, the energy calculation extension notebook used in conjunction with UTS [13] produced outputs for the nine experimental conditions in Table 4 with a different fuel type (Table 5). The drive cycle patterns for the ICEV scenario (Figure 7) are similar to those of the PHEV scenario (Figure 6). At an individual level, the outliers for both conditions (Figures 6 and 7) could be due to traffic congestion, vehicle weight and routes travelled. According to the vehicle's technical specification, [61], in extra-urban environments, the vehicle is claimed to do 5.1 L/100 km. Therefore, on average, the expected fuel consumption would be roughly 0.05 litres per kilometer (19.608 km/L), as described in the PHEV case, as adherence increases and driver behaviour is more compliant with rules. The energy consumption patterns are closer to the manufacturers' specification in Figure 7 for Experiment Conditions 3, 6 and 9. However, as adherence decreases, distance travelled increases, and the fuel consumption levels deviate from the vehicle manufacturer's technical specifications. This would be an expected behaviour as every vehicle is driving at various speeds (heterogenous driver behaviour), which is an unrealistic observation of driver behaviour. The vehicle manufacturer may not have considered this when estimating fuel consumption. It could be that the tests carried out to measure the fuel economy are conducted using specific drive cycles such as high adherence.

Two examples of simulated fuel types have been quantified with a reasonable degree of accuracy. This has resulted in enough data to quantify the costs of running these vehicles in the hypothetical urban street network.
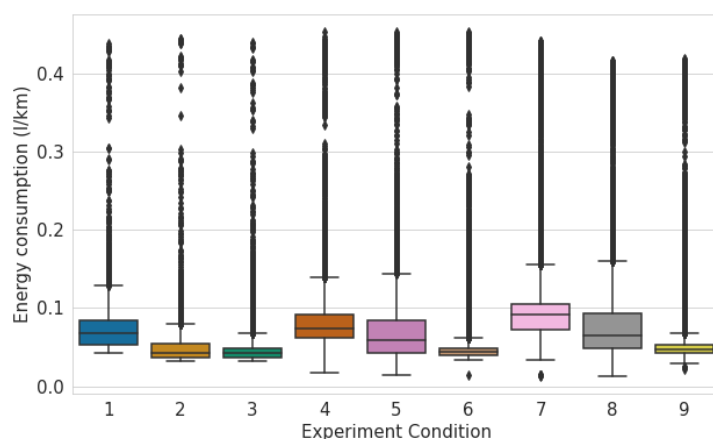

Figure 7. Box plots of energy consumption per kilometer (L/km) across all experiment conditions.

4.2.2. Monetary Costs of Fuel and Electric Consumption

The domestic cost of fuel per litre (L) and electricity per kilowatt-hour (kWh) fluctuates over time. The price for each varies, depending on vehicle fuel efficiency, distance travelled, weight and the fuel price [63]. Therefore, to quantify the cost in Great British Pounds (GBP), the current cost of petrol and electricity is adopted. These are GBP 1.43 (per L/km) [64] and GBP 0.17 (per kWh/km) [65], respectively.

To calculate the cost of petrol, the amount of petrol intake calculated for each vehicle was multiplied by 1.428, while the amount of electric energy intake was multiplied by 0.17. This produced a rough estimate of the fuel costs per car for each experiment condition for the UK.

The total cost of electric and petrol across all experiment conditions were £248.76 and £481.89, respectively (These costs are merely estimates produced from the vehicle-specific parameters seen in Tables 3 and 5 and drive cycle scenarios from Table 4 in an urban street network. These costs will not be the same in different types of street networks such as

highways, motorways and rural roads). Overall, it is £233.13 cheaper to run PHEVs over
ICEVs. As engine efficiency is greater for EV technologies [66], it is likely that these vehicles
would be more fuel-efficient and thus cost less than both PHEVs and ICEVs. In Figure 8,
a pattern emerges, where as driver adherence decreases (speeding increases) the cost of
electricity and petrol increases (experiment conditions 1, 4 and 7) relative to vehicle density.
Furthermore, as adherence increases, the difference in price between the fuel types shrinks
(experiment conditions 3, 6 and 9) as vehicles have travelled roughly the same distances
Figures 6 and 7. Similarly, these trends are broken down in the average cost per km in
Table A2. Overall, we observe that PHEVs on average are cheaper per kilometer travelled
than ICEVs. Furthermore, when the total cost of each model condition results are compared,
we see a clear distinction between costs, and overall, PHEVs are cheaper (Figure 8).
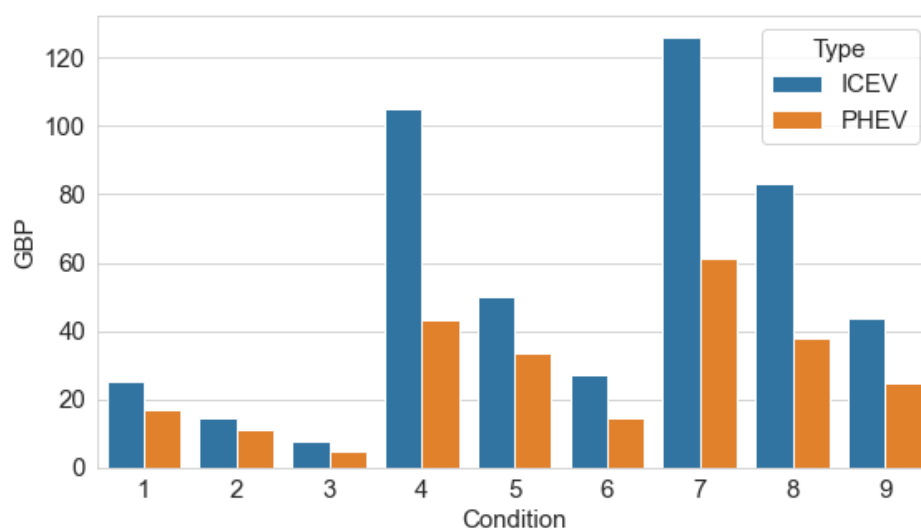

Figure 8. The total sum of petrol/electric costs (GBP) for each experiment condition across all vehicles.

A core strength of ABMs over mathematical models, as specified earlier, is the spatio-
temporal resolution variability of data. For instance, individual-level (vehicle-level) data
are attained and should provide a more enhanced snapshot of the impact behaviour had
on fuel costs.

An individual-level break-down of the fuel expenditure costs across all vehicles and
types are discerned in Figures 9 and 10 and in Appendix C.1, Figures A2–A5. These results
re-enforce our earlier made suppositions. For instance, as more vehicles regulate speed,
the difference in average costs decreases, as seen in Figures 9C and 10C. Despite these
trends, it could be argued that as variability amongst acceleration/deceleration increases
(heterogeneity), PHEV owners will save more money compared to ICEV owners. The net
benefits may not be substantial sums of money, but the environmental benefits (which have
not been modelled) could be a bonus for consumers. Furthermore, as empirical evidence
indicates, autonomous electric vehicles (AEVs) are more efficient than PHEVs/ICEVs [67].
Consequently, we could expect a greater extent of financial savings and environmental
benefits for owners of AEVs.

To conclude, when vehicle fleet is heterogeneous (more variability among speeds), this
leads to greater savings in adopting PHEVs over ICEVs as the engine efficiency is greater.
Consequently, more energy is converted to power than ICEVs (Experiment Conditions 4,
7). In contrast, as speeds become more regulated and similar, the average monetary costs
between the two vehicle types reduce, as seen in Figures 9C and 10C. Furthermore, these
findings are consistent for all fleet sizes, as seen in Figures A2F, A4F, A3I and A5I.
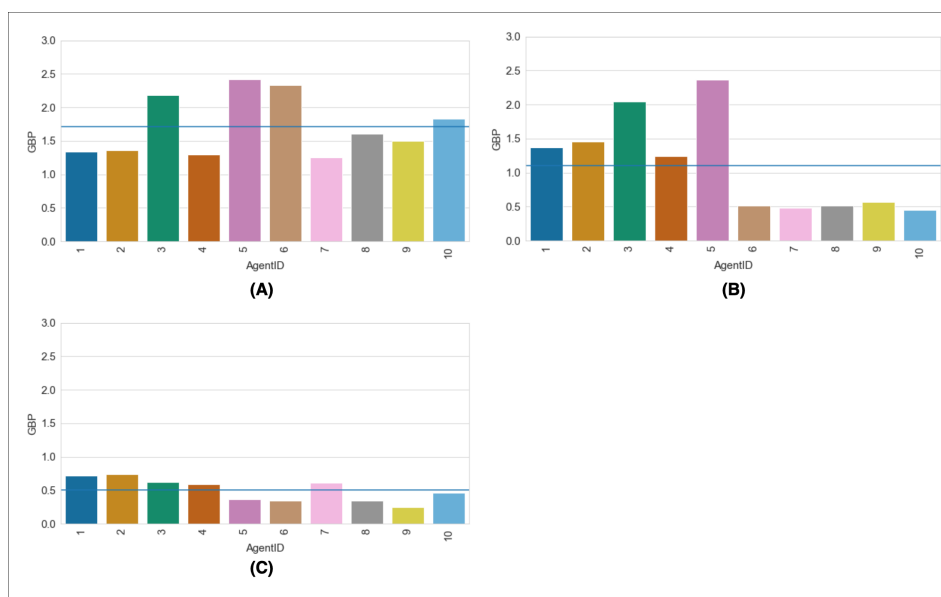
Figure 9. The total sum of electric costs (GBP) for each PHEV, model conditions 1 to 3. Where (**A**): 10 vehicles, 10 non-adherence, (**B**): 10 vehicles, 5 non-adherence and (**C**): 10 vehicles, 0 non-adherence.
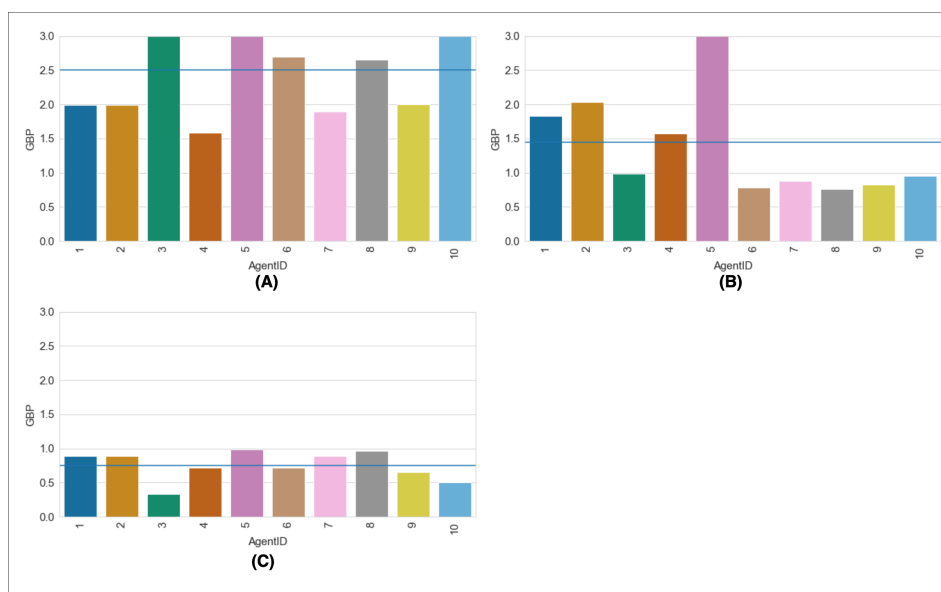

Figure 10. The total sum of petrol costs (GBP) for each ICEV, model conditions 1 to 3. Where (**A**): 10 vehicles, 10 non-adherence, (**B**): 10 vehicles, 5 non-adherence and (**C**): 10 vehicles, 0 non-adherence.

5. Discussion

This article set out to quantify the energy consumption by a fleet of vehicles in an urban street network using agent-based modelling. Given the current global agenda on climate change through various institutions and policies (i.e., COP 26, Paris Climate Accord 2015, Organisation for Economic Co-operation and Development, Green Economic Recovery (UK)), political discourse worldwide has shifted focus to green agendas, particularly renewable technologies, to facilitate a reduction of carbon emissions. The work conducted in this article plays a significant role in aiding national governments in modelling the potential landscape of energy consumption by EV/PHEVs. Previous literature has focused on mathematical models; however, this method is limited. Agent-based models are better suited to modelling individual-level drive cycle behaviours than mathematical models. The former typically provides an aggregated average of energy expenditure, while the latter provides a finer spatio-temporal resolution of individual-level energy consumption,

highlighting the immediate environment's impact on a vehicle's drive cycle, which affects energy consumption and efficiency. The model presented has demonstrated vehicle energy efficiency patterns that have been identified in empirical literature [57,58], namely that the longer distances travelled at speed reduces battery/engine efficiency, and conversely, vehicles that abide by rules in the long-term are more efficient. Another crucial finding was that as speed adherence increased, the energy consumption per kilometer better reflected vehicle manufacturer statistics for consumption; this was the case for both PHEV and ICEV tests, suggesting that vehicle manufacturers might be testing their vehicles at constant, more regulated speeds. Finally, we found that PHEVs overall are cheaper vehicles to run compared to ICEVs. This is due to several reasons, but primarily that PHEVs are more engine-efficient compared to ICEVs.

This work makes a novel methodological contribution to the modelling of vehicle energy consumption using agent-based modelling. While several attempts to model vehicle activity to quantify energy have been made, the majority of these models have hard-coded driver behaviour, which is bounded by constant speeds [54,68]. This, we believe, is not informative of energy consumption in urban spaces, where the stochastic environment plays a more significant role in affecting energy intake, such as urban speed limits, stop-go rules, and other vehicles in the street network.

Another vehicle technology that is beginning to gain traction is autonomous vehicles (AVs). UK Government projections show a net gain of 823,000 jobs and over £82 billion from the manufacturing and shipping of AVs [69]. AVs are likely to be electric, so their ascendance may also be considered in relation to electric energy usage of vehicles of the future. Ref. [67] outlines how AVs and electric vehicles may reduce energy consumption due to their connected environment, as route choice can be optimised to avoid congestion, undertake routes with fewer stops and ensure multiple passengers are catered to at once due to dynamic ride-sharing capabilities. Additionally, AVs may be able to drive in an optimally efficient manner due to the incorporation of traffic conditions received through communication and sensors. Ref. [67] estimates the energy consumption from these smoother driving cycles would decrease current energy use by between −10% and −20%.

In more revolutionary scenarios in which proportions of fully autonomous vehicles outweigh human-operated vehicles, vehicle-to-vehicle (V2V) communication could enable velocity synchronisation and shorter spaces between vehicles (i.e., platooning). Refs. [70,71] outline how this can improve string stability and increase network capacity as vehicles will operate with decreased acceleration noise and maintain closer distances to nearby vehicles, thus reducing aerodynamic drag. Ref. [67] outlines the energy and emissions reduction from autonomous vehicle platooning to be between 7% and 35%. Although sophisticated autonomous fleets (levels 4 and 5) are yet to be technologically perfected, as currently, the highest level of autonomy achieved in vehicles on sale is level 3 [72], these findings provide insight into the combined benefits of electric autonomous vehicle (EAV) fleets in the future.

6. Conclusions

A future avenue to explore would be to extend the model environment to cater for AVs. This should be achievable as the model can currently model specific vehicles and adherence levels. By modelling AVs, the variation of energy consumption scenarios of typical EVs and AVs can be compared. Furthermore, this could allow policymakers to model charging infrastructure in cities to test how these different vehicles can adapt optimally to these environmental changes.

A significant limitation of this work is computational tractability. The compute demand exponentially grows as we increase the number of vehicles or induce complex environmental settings. This can prevent users from simulating a greater capacity of vehicles or more complex cities. Secondly, we assume the world to be a flat plane in the model. However, this diverges from the real world. This assumption was due to computational demand, and we tried to configure the most simple environmental setting to ensure computation was not hampered. However, as cloud computing technologies become mainstream, this problem can be overcome.

Another limitation of this article is that it utilises an urban road typology only. While necessary, as most EV infrastructure is focused on cities, this does not necessarily imply that energy consumption from urban street networks would remain identical to other road typologies (e.g., motorways, dual-carriageways, rural roads). Therefore, in the future, the model can be extended by analysing vehicle behaviours and their subsequent impact on energy consumption in various road typologies.

This study highlights the importance of individual-based modelling methods such as ABMs in investigating future transport systems in cities. As some of the most important global policy agendas focus on the diffusion of low carbon-emitting technologies, this research is well-timed and crucial in planning for the future city.

Appendix A

Appendix A.1. Energy Calculation

To calculate the electricity energy consumption required to move the vehicles, the application of classical mechanics [74] including the drag equation from fluid dynamics [75] were adopted for this article.

When a vehicle is moving at a constant velocity, its forces are balanced (i.e., the forces driving it forward are equal to those resisting). However, vehicle velocity is not constant when driver behaviour changes over the drive cycle period (e.g., halting at traffic lights, matching the speed of vehicles ahead). Therefore, we assume velocity v is not constant in this model. A vehicle travelling at a non-constant speed results from an imbalance in the forces acting on it, i.e., the net force acting on the vehicle is non-zero. Considering the drive force from the engine, the force of gravity, the drag force and rolling resistance opposing motion, the net (or total) force acting on a vehicle, F_{total}, can be calculated as:

$$F_{total} = \overbrace{F}^{\text{drive}} - \overbrace{mg \times \sin(\theta)}^{\text{gravity}} - \overbrace{\frac{1}{2}\rho C_D A v^2}^{\text{drag}} - \overbrace{C_{rr} mg \times \cos(\theta)}^{\text{rolling resistance}}, \qquad \text{(A1)}$$

where:

- F is the force provided by the engine driving the vehicle forward (N);
- m is the mass of the vehicle (kg);
- g is the gravitational acceleration (m/s^2);

- θ is the angle of the surface on which the vehicle is driving on;
- ρ is the density of air (1.225 kg/m^3);
- C_D is the drag coefficient;
- A is the reference area of the vehicle (m^2) (width $\times$ height);
- v is the velocity (m/s), and;
- C_{rr} is the coefficient of rolling resistance.

For this investigation, the value of the coefficient of rolling resistance is taken to be 0.012 based on the assumption that all vehicles in the system are passenger vehicles and the road surfaces are made of smooth asphalt [76]. The total force acting on the vehicle can be expressed as the product of the vehicle's mass and its acceleration, i.e., $F_{total} = ma$, and consequently, we can write Equation (A1) as:

$$ma = F - mg \times \sin(\theta) - \frac{1}{2}\rho C_D A v^2 - C_{rr} mg \times \cos(\theta). \tag{A2}$$

In this investigation, we are concerned with the force produced by the engine, F, and the associated energy expended to produce this force. As a consequence, we may wish to rearrange Equation (A2) as:

$$F = ma + mg \times \sin(\theta) + \frac{1}{2}\rho C_D A v^2 - C_{rr} mg \times \cos(\theta). \tag{A3}$$

In the scenario where the road surface is flat, i.e., the vehicle is not travelling uphill or downhill, $\theta = 0$. This results in the gravitational aspect of the forces resisting motion being zero, i.e., $mg \sin(\theta) = 0$; it also results in the rolling resistance being $C_{rr} mg \times \cos(\theta) = C_{rr} mg$. Equation (A3) therefore becomes:

$$F = ma + \frac{1}{2}\rho C_D A v^2 + C_{rr} mg, \tag{A4}$$

which returns the force output by the car's engine to accelerate at rate a. In cases when the vehicle is travelling at a constant speed, Equation (A4) simplifies to:

$$F = \frac{1}{2}\rho C_D A v^2 + C_{rr} mg. \tag{A5}$$

Once the force exerted by the engine, F, and the distance of travel over which it is being exerted d are both known, the energy expended by the engine, E_{out}, can be calculated:

$$E_{out} = F \times d. \tag{A6}$$

In this case, E_{out} is the energy output by the engine. To find the energy provided to the engine in the form of fuel, the engine efficiency, k, is needed. Assuming that the efficiency of the engine is constant, i.e., that it has the same efficiency for all scenarios, the energy that needs to be provided to the engine can be found using the following equation:

$$E_{in} = F \times \frac{d}{k}, \tag{A7}$$

Appendix B

Tables

Table A1. Energy Calculation Extension notebook output data (EV/PHEV example).

Variable	Output Type
VelocityChange	Float
Acceleration	Float
Deceleration	Float
Braking Energy (kWh) [1]	Float
Drag_Force	Float
Acceleration_Force	Float
Total_Force	Float
Drag_Work	Float
Acceleration_Work	Float
Total_Work	Float
Energy_Input (kWh)	Float
Energy_Input_Sum (kWh)	Float

[1] An amount of energy is generated every time a vehicle brakes (decelerates), also known as regenerative braking. This is accounted for in the notebook using the braking energy formula from the following source: [77].

Table A2. Average cost (£) per km for both vehicle types.

MC	PHEV	ICEV
1	0.60	0.92
2	0.43	0.56
3	0.22	0.34
4	1.93	4.42
5	1.50	2.25
6	0.67	1.22
7	2.79	5.66
8	1.72	3.71
9	1.12	1.98

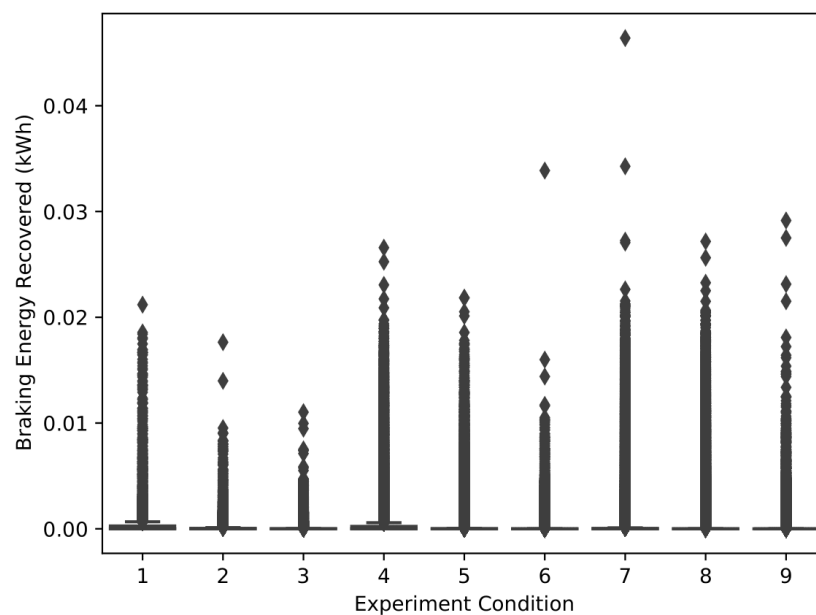## Appendix C

Appendix C.1. Figures

Figure A1. Box plots of braking energy recovered in kWh for each experiment condition.

Figure A2. The total sum of electric costs (GBP) for each PHEV, model conditions 4 to 6. Where (**D**): 50 vehicles, 50 non-adherence, (**E**): 50 vehicles, 25 non-adherence and (**F**): 50 vehicles, 0 non-adherence.

Figure A3. The total sum of electric costs (GBP) for each PHEV, model conditions 7 to 9. Where (**G**): 100 vehicles, 100 non-adherence, (**H**): 100 vehicles, 50 non-adherence and (**I**): 100 vehicles, 0 non-adherence
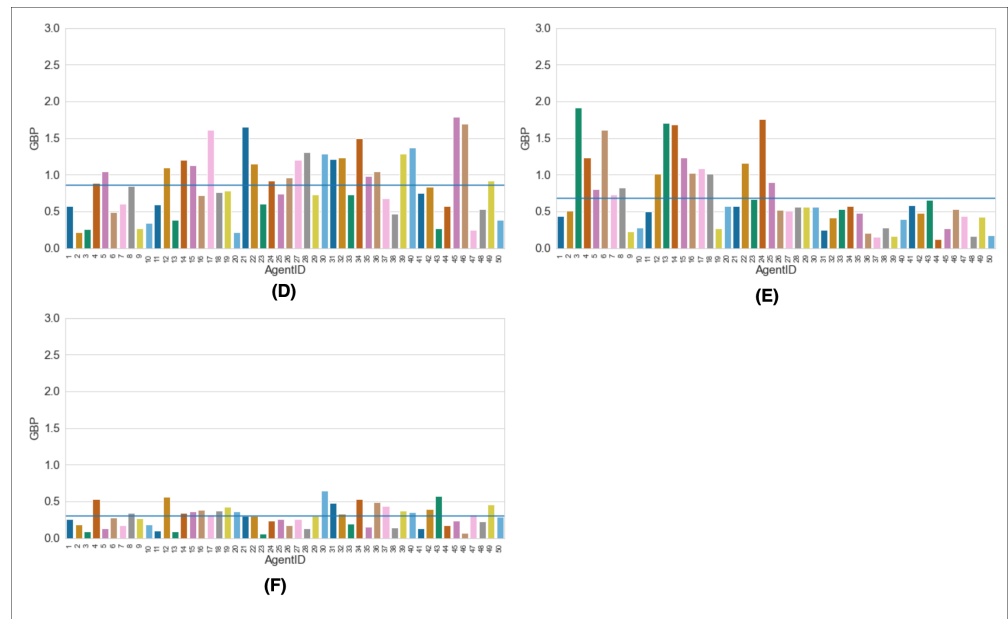
Figure A4. The total sum of petrol costs (GBP) for each ICEV, model conditions 4 to 6. Where (**D**): 50 vehicles, 50 non-adherence, (**E**): 50 vehicles, 25 non-adherence and (**F**): 50 vehicles, 0 non-adherence.
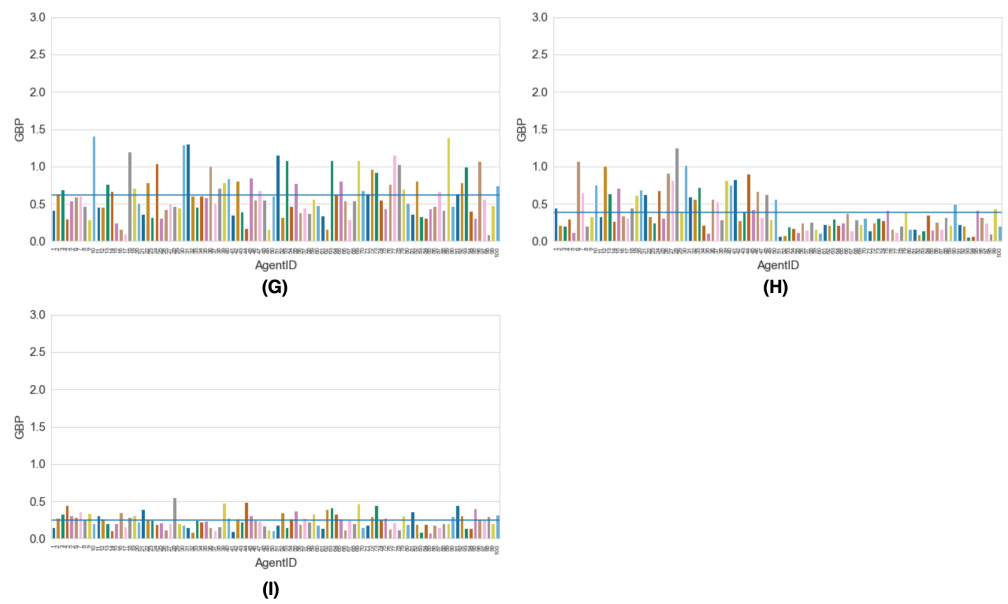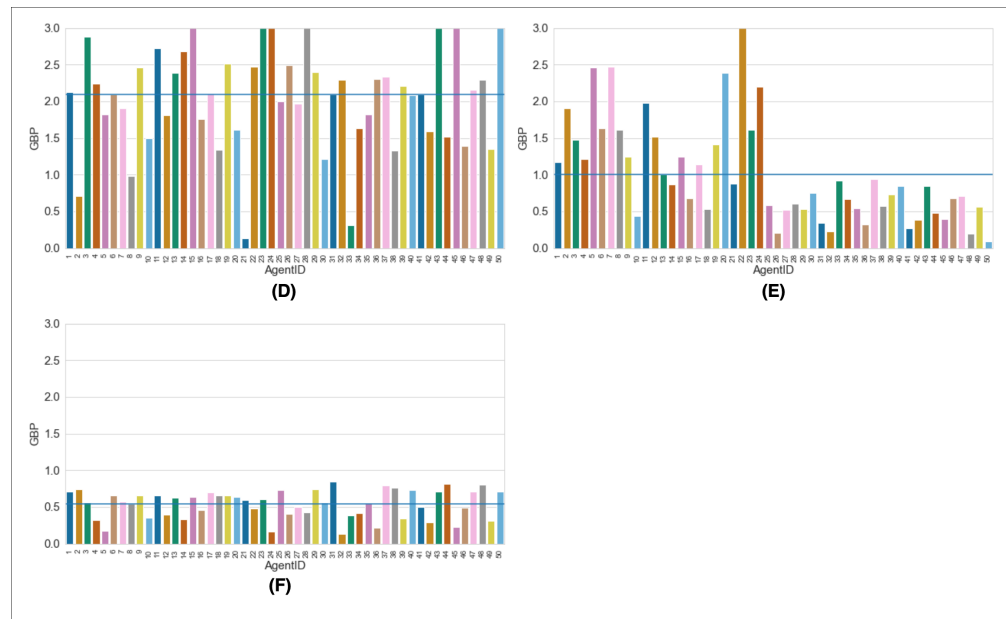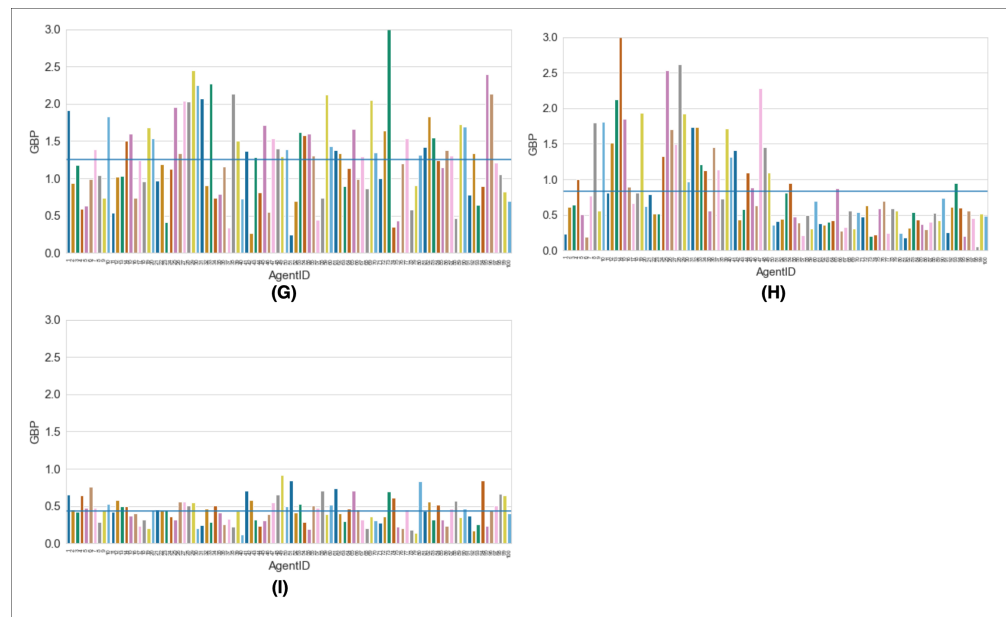

Figure A5. The total sum of petrol costs (GBP) for each ICEV, model conditions 7 to 9. Where (**G**): 100 vehicles, 100 non-adherence, (**H**): 100 vehicles, 50 non-adherence and (**I**): 100 vehicles, 0 non-adherence

References

1. Bretzke, W.R. Global urbanization: A major challenge for logistics. *Logist. Res.* **2013**, *6*, 57–62. [CrossRef]
2. Dhakal, T.; Min, K.S. Macro Study of Global Electric Vehicle Expansion. *Foresight STI Gov.* **2021**, *15*, 67–73. [CrossRef]
3. London Assembly. Electric Vehicle Infrastructure | London City Hall. Available online: https://www.london.gov.uk/what-we-do/environment/pollution-and-air-quality/electric-vehicle-infrastructure (accessed on 13 October 2021).
4. Albatayneh, A.; Assaf, M.N.; Alterman, D.; Jaradat, M. Comparison of the Overall Energy Efficiency for Internal Combustion Engine Vehicles and Electric Vehicles. *Environ. Clim. Technol.* **2020**, *24*, 669–680. [CrossRef]
5. Sierzchula, W.; Bakker, S.; Maat, K.; Van Wee, B. The competitive environment of electric vehicles: An analysis of prototype and production models. *Environ. Innov. Soc. Transit.* **2012**, *2*, 49–65. [CrossRef]
6. Sarlioglu, B.; Morris, C.T.; Han, D.; Li, S. Driving Toward Accessibility: A Review of Technological Improvements for Electric Machines, Power Electronics, and Batteries for Electric and Hybrid Vehicles. *IEEE Ind. Appl. Mag.* **2017**, *23*, 14–25. [CrossRef]

7. Tan, X.; Zeng, Y.; Gu, B.; Wang, Y.; Xu, B. Scenario Analysis of Urban Road Transportation Energy Demand and GHG Emissions in China—A Case Study for Chongqing. *Sustainability* **2018**, *10*, 2033. [CrossRef]

8. Wang, K.; Ke, Y. Public-Private Partnerships in the Electric Vehicle Charging Infrastructure in China: An Illustrative Case Study. *Adv. Civ. Eng.* **2018**, *2018*, 9061647. [CrossRef]

9. Angus, T. 2021 Australian Energy Statistics (Electricity) | Ministers for the Department of Industry, Science, Energy and Resources; Ministers for the Department of Industry, Science, Energy and Resources 2021. Available online: https://www.minister.industry. gov.au/ministers/taylor/media-releases/2021-australian-energy-statistics-electricity (accessed on 5 October 2021).

10. Hawkins, T.R.; Gausen, O.M.; Strømman, A.H. Environmental impacts of hybrid and electric vehicles—A review. *Int. J. Life Cycle Assess.* **2012**, *17*, 997–1014. [CrossRef]

11. Global Warming Potential—An Overview | ScienceDirect Topics. 2021. Available online: https://www.sciencedirect.com/topics/ engineering/global-warming-potential (accessed on 30 March 2021).

12. Hawkins, T.R.; Singh, B.; Majeau-Bettez, G.; Strømman, A.H. Comparative environmental life cycle assessment of conventional and electric vehicles. *Wiley Online Libr.* **2013**, *17*, 53–64. [CrossRef]

13. Olmez, S.; Sargoni, O.; Heppenstall, A.; Birks, D.; Whipp, A.; Manley, E. 3D Urban Traffic Simulator (ABM) in Unity. Available online: https://www.comses.net/codebases/32e7be8c-b05c-46b2-9b5f-73c4d273ca59/releases/1.1.0/ (accessed on 23 March 2021).

14. Xing, Y.; Lv, C.; Cao, D. Driver Behavior Recognition in Driver Intention Inference Systems. *Adv. Driv. Intent. Inference* **2020**, *258*, 99–134. [CrossRef]

15. Huston, M.; DeAngelis, D.; Post, W. New Computer Models Unify Ecological Theory. *BioScience* **1988**, *38*, 682–691. [CrossRef]

16. Birks, D.; Townsley, M.; Stewart, A. Generative explanations of crime: Using simulation to test criminological theory. *Criminology* **2012**, *50*, 221–254. [CrossRef]

17. Malleson, N.; Heppenstall, A.; See, L. Crime reduction through simulation: An agent-based model of burglary. *Comput. Environ. Urban Syst.* **2010**, *34*, 236–250. [CrossRef]

18. Heckbert, S.; Baynes, T.; Reeson, A. Agent-based modeling in ecological economics. *Ann. N. Y. Acad. Sci.* **2010**, *1185*, 39–53. [CrossRef]

19. McLane, A.J.; Semeniuk, C.; McDermid, G.J.; Marceau, D.J. The role of agent-based models in wildlife ecology and management. *Ecol. Model.* **2011**, *222*, 1544–1556. [CrossRef]

20. Filatova, T.; Verburg, P.H.; Parker, D.C.; Stannard, C.A. Spatial agent-based models for socio-ecological systems: Challenges and prospects. *Environ. Model. Softw.* **2013**, *45*, 1–7. [CrossRef]

21. Olner, D.; Evans, A.; Heppenstall, A. An agent model of urban economics: Digging into emergence. *Comput. Environ. Urban Syst.* **2015**, *54*, 414–427. [CrossRef]

22. Dawid, H.; Neugart, M. Agent-based models for economic policy design. *East. Econ. J.* **2011**, *37*, 44–50. [CrossRef]

23. Squazzoni, F. *Agent-Based Computational Sociology*; John Wiley & Sons: New York, NY, USA, 2012. [CrossRef]

24. Bianchi, F.; Squazzoni, F. Agent-based models in sociology. *WIREs Comput. Stat.* **2015**, *7*, 284–306. [CrossRef]

25. Heppenstall, A.J.; Crooks, A.T.; See, L.M.; Batty, M. *Agent-Based Models of Geographical Systems*; Springer: Cham, The Netherlands, 2012; pp. 1–759. [CrossRef]

26. Crooks, A. Agent-Based Models and Geographical Information Systems. In *Geocomputation: A Practical Primer*; Sage: Thousand Oaks, CA, USA, 2015; pp. 63–77.

27. Thompson, J.; Read, G.J.; Wijnands, J.S.; Salmon, P.M. The perils of perfect performance; considering the effects of introducing autonomous vehicles on rates of car vs. cyclist conflict. *Ergonomics* **2020**, *63*, 981–996. [CrossRef]

28. Olmez, S.; Douglas-Mann, L.; Manley, E.; Suchak, K.; Heppenstall, A.; Birks, D.; Whipp, A. Exploring the Impact of Driver Adherence to Speed Limits and the Interdependence of Roadside Collisions in an Urban Environment: An Agent-Based Modelling Approach. *Appl. Sci.* **2021**, *11*, 5336. [CrossRef]

29. Davis, G.A.; Morris, P. Statistical versus Simulation Models in Safety: Steps Toward a Synthesis Using Median-Crossing Crashes. *Transp. Res. Rec.* **2009**, *2102*, 93–100. [CrossRef]

30. Kangur, A.; Jager, W.; Verbrugge, R.; Bockarjova, M. An agent-based model for diffusion of electric vehicles. *J. Environ. Psychol.* **2017**, *52*, 166–182. [CrossRef]

31. Eppstein, M.J.; Grover, D.K.; Marshall, J.S.; Rizzo, D.M. An agent-based model to study market penetration of plug-in hybrid electric vehicles. *Energy Policy* **2011**, *39*, 3789–3802. [CrossRef]

32. Hasan, M.A.; Frame, D.J.; Chapman, R.; Archie, K.M. Costs and emissions: Comparing electric and petrol-powered cars in New Zealand. *Transp. Res. Part D Transp. Environ.* **2021**, *90*, 102671. [CrossRef]

33. Palmer, K.; Tate, J.E.; Wadud, Z.; Nellthorp, J. Total cost of ownership and market share for hybrid and electric vehicles in the UK, US and Japan. *Appl. Energy* **2018**, *209*, 108–119. [CrossRef]

34. Bencivenga, C.; Sargenti, G.; D'Ecclesia, R.L. Energy markets: Crucial relationship between prices. *Math. Stat. Methods Actuar. Sci. Financ.* **2010**, 23–32. [CrossRef]

35. Iea. Electricity Market Report—December 2020—Analysis—IEA. Available online: https://www.iea.org/reports/electricity-market-report-december-2020 (accessed on 8 December 2021).

36. Letmathe, P.; Suares, M. A consumer-oriented total cost of ownership model for different vehicle types in Germany. *Transp. Res. Part D Transp. Environ.* **2017**, *57*, 314–335. [CrossRef]

37. Grimm, V.; Berger, U.; Bastiansen, F.; Eliassen, S.; Ginot, V.; Giske, J.; Goss-Custard, J.; Grand, T.; Heinz, S.K.; Huse, G.; et al. A standard protocol for describing individual-based and agent-based models. *Ecol. Model.* **2006**, *198*, 115–126. [CrossRef]

38. Speed Limits—GOV.UK. 2021. Available online: https://www.gov.uk/speed-limits (accessed on 30 March 2021).

39. How Much Does a Car Weigh? [Average by Car Model & Type]. 2021. Available online: https://mechanicbase.com/cars/car-weight/ (accessed on 30 March 2021).

40. Balendra, P. *Vehicle Speed Compliance Statistics, Great Britain: January–June 2020*; Technical Report; Department for Transport: London, UK, 2020.

41. Juliani, A.; Berges, V.P.; Vckay, E.; Gao, Y.; Henry, H.; Mattar, M.; Lange, D. Unity: A general platform for intelligent agents. *arXiv* **2018**, arXiv:1809.02627.

42. Han, B.; Sun, D.; Yu, X.; Song, W.; Ding, L. Classification of urban street networks based on tree-like network features. *Sustainability* **2020**, *12*, 628. [CrossRef]

43. Boeing, G. A multi-scale analysis of 27,000 urban street networks: Every US city, town, urbanized area, and Zillow neighborhood. *Environ. Plan. B Urban Anal. City Sci.* **2020**, *47*, 590–608. [CrossRef]

44. Porta, S.; Crucitti, P.; Latora, V. The network analysis of urban streets: A dual approach. *Phys. Stat. Mech. Its Appl.* **2006**, *369*, 853–866. [CrossRef]

45. Filocamo, B.; Ruiz, J.A.; Sotelo, M.A. Efficient management of road intersections for automated vehicles-the FRFP system applied to the various types of intersections and roundabouts. *Appl. Sci.* **2020**, *10*, 316. [CrossRef]

46. Thompson, J.; Stevenson, M.; Wijnands, J.S.; Nice, K.A.; Aschwanden, G.D.; Silver, J.; Nieuwenhuijsen, M.; Rayner, P.; Schofield, R.; Hariharan, R.; et al. A global analysis of urban design types and road transport injury: An image processing study. *Lancet Planet. Health* **2020**, *4*, e32–e42. [CrossRef]

47. Department for Transport. *Setting Local Speed Limits*; Technical Report July; UK Government Department for Transport: London, UK, 2006. Available online: https://www.gov.uk/government/publications/setting-local-speed-limits/setting-local-speed-limits (accessed on 20 October 2021).

48. Heppenstall, A.; Evans, A.; Birkin, M. Using hybrid agent- based systems to model spatially—Influenced retail markets. *J. Artif. Soc. Soc. Simul.* **2006**, *9*.

49. Kothari, V.; Blythe, J.; Smith, S.; Koppel, R. *Agent-Based Modeling of User Circumvention of Security*; ACM International Conference Proceeding Series; ACM: Paris, France, 2014. [CrossRef]

50. Benenson, I.; Martens, K.; Birfir, S. PARKAGENT: An agent-based model of parking in the city. *Comput. Environ. Urban Syst.* **2008**, *32*, 431–439. [CrossRef]

51. Sert, E.; Bar-Yam, Y.; Morales, A.J. Segregation dynamics with reinforcement learning and agent based modeling. *Sci. Rep.* **2020**, *10*, 11771. [CrossRef]

52. Thompson, J.H.; Wijnands, J.S.; Mavoa, S.; Scully, K.; Stevenson, M.R. Evidence for the 'safety in density' effect for cyclists: validation of agent-based modelling results. *Inj. Prev.* **2019**, *25*, 379–385. [CrossRef]

53. Gaete-Morales, C.; Kramer, H.; Schill, W.P.; Zerrahn, A. An open tool for creating battery-electric vehicle time series from empirical data—Emobpy. *Sci. Data* **2020**, *8*, 152. [CrossRef]

54. Gaete-Morales, C. Emobpy: Application for the German Case, 2021, Open Access, Dataset. Available online: https://zenodo.org/record/4514928 (accessed on 23 March 2021).

55. Electric Vehicle Market Statistics 2021—How Many Electric Cars in UK? 2021. Available online: https://www.nextgreencar.com/electric-cars/statistics/ (accessed on 22 September 2021).

56. Brslica, V. Plug-in Hybrid Vehicles. *Electr. Veh. Benefits Barriers* **2011**. [CrossRef]

57. Moriarty, P.; Wang, S.J. Can Electric Vehicles Deliver Energy and Carbon Reductions? *Energy Procedia* **2017**, *105*, 2983–2988. [CrossRef]

58. Wager, G.; Whale, J.; Braunl, T. Driving electric vehicles at highway speeds: The effect of higher driving speeds on energy consumption and driving range for electric vehicles in Australia. *Renew. Sustain. Energy Rev.* **2016**, *63*, 158–165. [CrossRef]

59. Outlander, M. Running Costs—Mitsubishi Outlander PHEV | Cut your Costs. 2021. Available online: https://www.mitsubishi-motors.ie/cars/outlander-phev/cost (accessed on 30 September 2021).

60. Best-Selling Cars in the UK 2020 | Auto Express. 2021. Available online: https://www.autoexpress.co.uk/news/354230/best-selling-cars-uk-2020 (accessed on 20 October 2021).

61. All-New Ford Fiesta st Specifications Performance and Economy. Available online: https://media.ford.com/content/dam/fordmedia/Europe/documents/productReleases/Fiesta/2018FordFiesta_ST_TechSpecs_EU.pdf (accessed on 20 October 2021).

62. How Efficient Is Your Cars Engine | AAA Automotive. 2021. Available online: https://www.aaa.com/autorepair/articles/how-efficient-is-your-cars-engine (accessed on 27 October 2021).

63. Shafiei, E.; Leaver, J.; Davidsdottir, B. Cost-effectiveness analysis of inducing green vehicles to achieve deep reductions in greenhouse gas emissions in New Zealand. *J. Clean. Prod.* **2017**, *150*, 339–351. [CrossRef]

64. United Kingdom Gasoline Prices, 25-October-2021 | GlobalPetrolPrices.com. 2021. Available online: https://www.globalpetrolprices.com/United-Kingdom/gasoline{_}prices/ (accessed on 27 October 2021).

65. Cost of Charging an Electric Car | Pod Point. 2021. Available online: https://pod-point.com/guides/driver/cost-of-charging-electric-car (accessed on 27 October 2021).

66. Prud'homme, R.; Koning, M. Electric vehicles: A tentative economic and environmental evaluation. *Transp. Policy* **2012**, *23*, 60–69. [CrossRef]

67. Lee, J.; Kockelman, K.M. Energy implications of self-driving vehicles. In Proceedings of the 98th Annual Meeting of the Transportation Research Board, Washington, DC, USA, 13–17 January 2019.

68. Butler, K.L.; Ehsani, M.; Kamath, P. A matlab-based modeling and simulation package for electric and hybrid electric vehicle design. *IEEE Trans. Veh. Technol.* **1999**, *48*, 1770–1778. [CrossRef]

69. Places Catapult, C. *Connected Places Catapult Market Forecast For Connected and Autonomous Vehicles*; Catapult: UK. Available online: https://assets.publishing.service.gov.uk/government/uploads/system/uploads/attachment_data/file/919260/connected-places-catapult-market-forecast-for-connected-and-autonomous-vehicles.pdf (accessed on 30 October 2021).

70. Li, S.E.; Zheng, Y.; Li, K.; Wu, Y.; Hedrick, J.K.; Gao, F.; Zhang, H. Dynamical Modeling and Distributed Control of Connected and Automated Vehicles: Challenges and Opportunities. *IEEE Intell. Transp. Syst. Mag.* **2017**, *9*, 46–58. [CrossRef]

71. Talebpour, A.; Mahmassani, H.S. Influence of connected and autonomous vehicles on traffic flow stability and throughput. *Transp. Res. Part C Emerg. Technol.* **2016**, *71*, 143–163. [CrossRef]

72. New Level 3 Autonomous Vehicles Hitting the Road in 2020—IEEE Innovation at Work. Available online: https://innovationatwork.ieee.org/new-level-3-autonomous-vehicles-hitting-the-road-in-2020/ (accessed on 22 October 2021).

73. Olmez, S.; Heppenstall, A. *Drive Cycle Data from the 3D Urban Traffic Simulator (ABM) in Unity (Version 1.1.0)*; Figshare: London, UK, 2021. [CrossRef]

74. Kibble, T.; Berkshire, F. *Classical Mechanics*; World Scientific Publishing Company: Singapore, 2004.

75. Batchelor, C.; Batchelor, G. *An Introduction to Fluid Dynamics*; Cambridge University Press: Cambridge, UK, 2000.

76. Pałasz, B.; Waluś, K.J.; Warguła, L. The determination of the rolling resistance coefficient of a passenger vehicle with the use of roller test bench method. *MATEC Web Conf.* **2019**, *254*, 04007. [CrossRef]

77. Ram, A. Braking Energy Calculation for a Given Drive Cycle and Different Methods of Regenerative Braking: Skill-Lync. Available online: https://skill-lync.com/student-projects/week-11-challenge-braking-6 (accessed on 22 December 2021).